Article:
Sun, Q, Chen, C, Kemp, AH et al. (1 more author) (2021) An on-board detection framework for polygon wear of railway wheel based on vibration acceleration of axle-box. Mechanical Systems and Signal Processing, 153. 107540. ISSN 0888-3270

https://doi.org/10.1016/j.ymssp.2020.107540

An on-board detection framework for polygon wear of railway wheel based on vibration acceleration of axle-box

Qi Sun[a], Chunjun Chen[a,b], Andrew H. Kemp[c], Peter Brooks[c]

a. School of Mechanical Engineering, Southwest Jiaotong University, Chengdu, Sichuang, China

b. Technology and equipment of rail Transit Operation and maintenance key laboratory of Sichuan province, Southwest Jiaotong University, Chengdu, Sichuang, China

c. Institute for High Speed Rail and System Integration, University of Leeds, Leeds, UK

Abstract: The polygon wear of railway wheel (PWRW) is a wear fault that is ubiquitous in railway vehicles. PWRW can induce a strong periodic excitation to both vehicle and track, which not only decreases passenger comfort but also is detrimental to the operational reliability and safety. Both the degree and the order of PWRW are important parameters used to quantify the fault. Because the fault-related components distribute at a wide range in the frequency domain, it is easy to alias with some radiated vibrations from vehicle and track components, which makes the on-board detection for both parameters of PWRW very difficult. To address the practical engineering problem, this paper proposes a detection framework based on the angle domain synchronous averaging technique (ADSAT). The detection method employs the vertical axle-box vibration acceleration (ABVA), which is easy to obtain and can also be used to monitor the conditions of axle-box bearings. The paper compares the proposed and traditional methods. The results reveal that the proposed method not only achieves the order detection which the traditional method cannot, but also mitigates the influence of background noise. The feasibility and effectiveness of the proposed method to improve the detection accuracy of PWRW is demonstrated through simulation and real field investigations.

Key word: railway wheel polygonization; rotating machine fault diagnosis; angle domain synchronous averaging technique; axle-box vibration acceleration;

1. Introduction

Steel railway wheels in service invariably wear, which contributes to out-of-roundness (OOR) imperfections such as isolated flats and tread polygonization. Research on the tread polygonization fault has been undertaken since last century[1][2]. In 1999, Meinke[3] proposed a dynamics model with 40-DOF to explain the process of railway wheel tread polygonization. The study mainly focused on the effects of the gyroscopic and inertial moments of wheels to PWRW. In 2000, Nielsen[4] defined the difference between polygon wear and other forms of OOR in railway wheels. They studied the generation mechanism of 1^{st}-5^{th} order PWRW and proposed a wheel re-profiling standard as well as some strategies to reduced PWRW. However, their strategies cannot be applied to all situations. In 2005, Johansson[5] established a three-dimensional multi-body system model of wheel-rail interaction considering wheel-rail wear based on the FASTSIM algorithm. The model was used to simulate the dynamics of the wheels with 1^{st}-20^{th} order polygon tread separately. In 2012, Jin[6] analyzed the generation mechanism of polygon wear of subway vehicles by the modal analysis method. They found that the first-order bending frequency of the wheelset is same as the passing frequency of 9^{th} order PWRW. They proposed that enlarging radius of wheelset shaft can

eliminate the polygonization phenomena of subway vehicles. However, the causes of PWRW are diverse which include disc brakes[1], wheelset bending modes[2], clamping methods during re-profiling procedures[4], P2 resonance[5], unsprung mass[7] and so on. The order of wheel polygonization for a single wheel is variable, which makes the causes analysis more difficult.

PWRW has many detrimental influences on vehicle-track systems and passenger comfort. In 2014, Jie[8] studied the influence of PWRW on the interior noise of high-speed trains based on hybrid finite element and statistic energy analysis (FE-SEA) method. Their research showed that wheel polygon wear had a great impact on interior noise and that wheels with different order of polygon wear and the same roughness levels can cause different noises. The higher order polygon wear has the more serious consequences on passenger comfort so that the order is important parameter to represent the fault of PWRW. In 2016, Bogacz[9] studied the effect of PWRW on the vertical wheel-rail force of train vehicles. Their research showed that a train with a polygon wheel can easily reach its critical speed and can even derail, whilst running at moderate speeds. PWRW also increases the risk of rail breaks, sleeper cracking, axle damage, bearing damage and so on[10]. Therefore, it is desirable to monitor the health status of PWRW in time.

Many works on the generation mechanism and the influence of PWRW have been studied, but few are related to the on-board detection technology of PWRW. In 2013, Ding[11] proposed to extract a time-frequency indicator for evaluating the wheel OOR based on frequency slice wavelet transform (FSWT) and verified the effectiveness based on simulated data. However, the method was not used to be proved by any real field data and cannot recognize the order of PWRW. In 2016, Yifan[12] proposed a method based on Hilbert-Huang Transform (HHT) to detect the OOR of railway wheels. This method requires empirical mode decomposition (EMD), which has a significant calculation cost. Therefore, the method cannot be easily used to monitor the wheel health condition in on-board. In 2018, Qi[13] proposed a method to detect the fault of PWRW according to wavelength-fixing generation mechanism that PWRW caused by the fixed distance between two adjacent rail sleepers . The effectiveness was verified by real field data, but the method is not suitable for all conditions of PWRW. In 2019, Xu[14] proposed an automatic detection method based generalized resonance demodulation method. They believed that railway wheel polygonization induces impulsive excitation to tracks and vehicles rather than harmonic excitation. In 2020, Wang[15] proposed an on-board detection method by using Bayesian forecasting and dynamic model but it can’t come true the detection of the order of wheel polygonization.

PWRW has become an urgent problem to address in high-speed railways[16]. Some certain lines matching with certain vehicles are extremely easy to occur wheel polygonization. To solve the issue, maintenance departments always adopt the excessively frequent wheel re-profiling and intensive manual measurement. These strategies not only reduce the service life of wheels but also require excess human resource. In summary, there is currently no on-board detection algorithm that is simple, highly versatile, reliable, low cost and independent of the track or vehicle structures monitoring the PWRW. On the other hand, the continuous development of high-speed train technology, particularly in China, using holographic systems for monitoring railway vehicle mechanical parts is gradually become more commonplace. All of these make it imperative to design and implement an on-board detection system for PWRW. This paper proposes a novel on-board detection framework for PWRW based on vertical axle-box vibration acceleration (ABVA) with the angle domain synchronous averaging technique (ADSAT). This method meets the requirements of accuracy, stability and speed for on-board monitoring of detecting the structural fault of PWRW.

2. Dynamic performance of PWRW

2.1. Polygon wear of railway wheel

The OOR of railway wheel is divided into global defects and local defects. Local defects are discrete, such as wheel flats, which generate impulse excitation to vehicles and tracks[17]. PWRW is a main type of global tread defects and is defined as a periodic deviation, formed by uneven wear in the circumferential direction[18]. A wheel with polygon wear is shown in Figure 1.

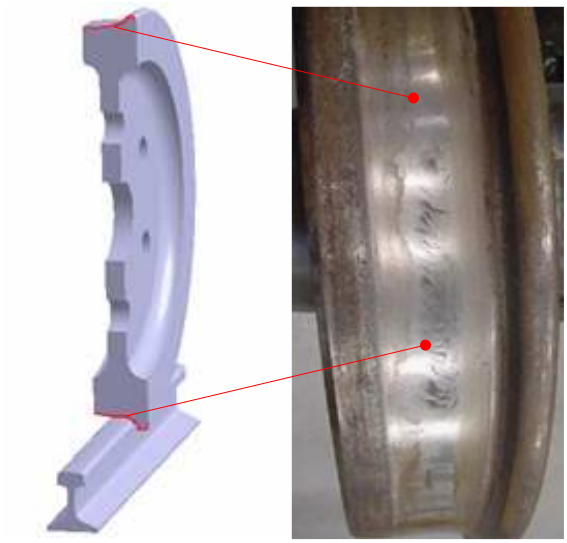

Figure 1 Polygon wheel tread

Generally, the quantitative characterization of PWRW is expressed in polar coordinates. There are three parameters to describe polygon wear on a wheel, which are the roughness, the order and the phase. An illustration of the three parameters is shown in Figure 2: (a) the roughness level parameter of PWRW describes the peak-to-peak value of geometrical irregularities of wheel tread, (b) the order parameter of PWRW represents how many wavelengths within one wheel circumference, and (c) the phase parameter of PWRW represents the phase shift between the left and the right wheels on a wheelset. The greater phase shifts mean the faster the wheels exhibit OOR[1]. For a single wheel, there are just two parameters to represent PWRW, the roughness level and the polygonal order.

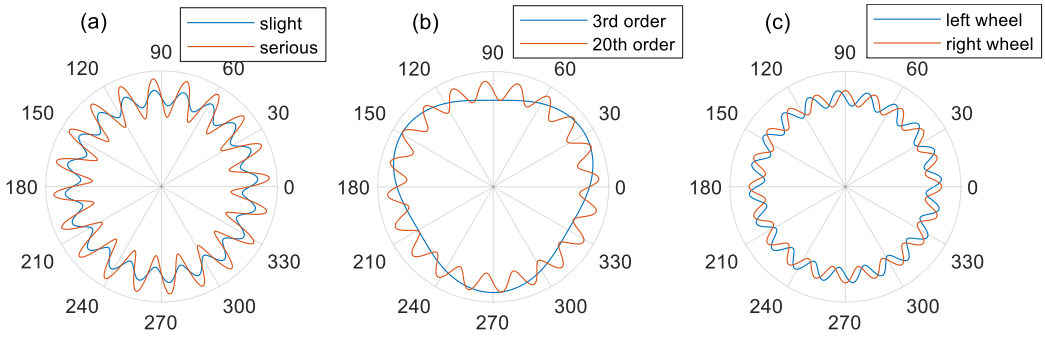

Figure 2 Different examples of wheels with polygonal wear

The roughness level of PWRW can be calculated based on the measured profile deviation from the mean wheel radius[17], as:

$$L_\theta = 20\log_{10}\left(\frac{\tilde{r}_\theta}{r_{ref}}\right) \tag{1}$$

where L_θ is the roughness level of θ^{th} order PWRW, $\tilde{r}_\theta$ is the RMS in 1/3 octave bands with center frequency f_θ of power spectral density (PSD) of measured profile deviation, a reference value $r_{ref} = 1\mu m$. The center wavelength λ_θ corresponds to the order of PWRW by:

$$\theta = \frac{c}{\lambda_\theta} \tag{2}$$

where c stands for the nominal wheel circumference.

2.2. Dynamic performance of PWRW

In general, PWRW induces several narrowband harmonic excitations, of significant amplitude, in tracks and vehicles through wheel-rail contact. The displacement function $z(t)$ of the excitation model of PWRW is given by[18]:

$$Z(t) = \sum_{\theta=1}^{H} A_\theta \sin\left[\theta\left(\frac{v/3.6}{R}\right)t + \varphi_\theta\right] \tag{3}$$

where $z(t)$ is the displacement excitation, θ is the order, t is the time, H is the maximum of the order, typical H=40, v is the forward speed of vehicle, R is the nominal wheel radius, A_θ is the amplitude of the harmonic vibration caused by the θ^{th}-order polygon wear which responds to the roughness level, φ_θ is the original phase of the harmonic vibration caused by the θ^{th}-order polygon wear. The fundamental passing frequency of PWRW is the wheel rotational frequency, so that the θ^{th}-order fault-related feature frequencies are:

$$f_\theta = \theta f_0 = \theta\frac{v/3.6}{2\pi R} \tag{4}$$

Normally, several different PWRW orders exist simultaneously. In this paper, only the dominant order is the critical parameter. PWRW can cause high vertical force and noise by wheel-rail interactions[2], which radiates to affect the increasing of the vibration in the axle-box[19]. More specifically, the Root Mean Square (RMS) value of the ABVA with a polygonal wheel will reach 20g to 40g, while a value of is less than 5g as usual.

3. Detection methods for PWRW

The detection technologies of PWRW are divided into direct measurements and indirect measurements. The direct methods often have higher accuracy but they require the train to be stable or running at extremely low speed[20]. Hence, direct methods are not easy to be carried out by on-board detection. In general, the on-board detection process of mechanical structural health diagnosis involves four steps, namely data acquisition (DAQ), feature extraction, classification and maintenance decision. Normally, shaft temperature, wheel-rail contact force, sound, vibration, ultrasonic and acoustic signals can be used to monitor mechanical wheel health state[21]. However, temperature signals cannot capture the incipient wheel faults. Sound signals are easily influenced by environmental sound noise. Wheel-rail force signals are not easily obtained. Vibration signals can capture the mechanical structural incipient faults and have higher stability for mechanical structural health monitoring (SHM). The axle-box is the nearest stationary mechanical structure. So

that the proposed detection method of PWRW are based on vibration signals emanating from railway vehicle axle-boxes. The monitoring point is shown as Figure 3.

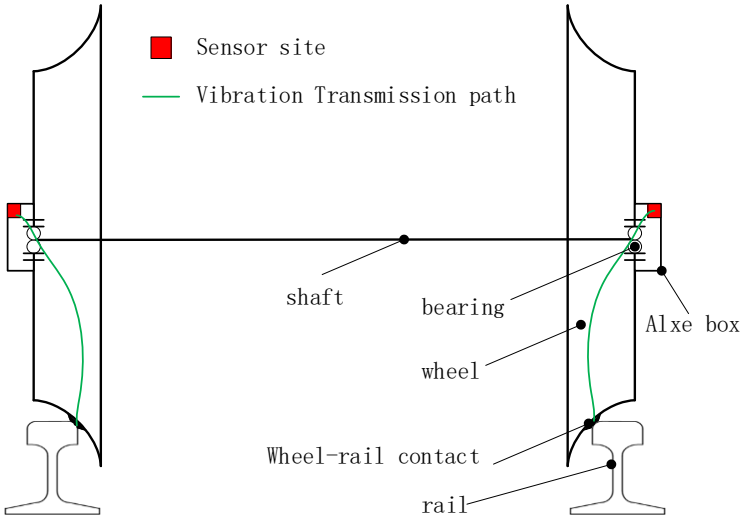

Figure 3 The monitoring point based on ABVA

3.1. Traditional diagnosis method

The traditional method to detect the fault of PWRW relies on the use of a Discrete-time Fourier transform (DTFT) of the ABVA $y(n)$: [18]

$$Y(k)=\sum_{n=0}^{N-1} y(n)e^{-2\pi jn\frac{k-1}{N}} \tag{5}$$

Where $Y(k)$ is the DTFT of $y(n)$, k is a is a series of natural numbers which correspond to the discrete frequencies f ($=kf_{vs}/N$), f_{vs} is the sampling frequency of the monitoring vibration data, j is Imaginary unit. N is the discrete points number of $y(n)$. The roughness level of PWRW is represented by:

$$TZ_d = \max_{1\le k<\frac{N}{2}} \left|Y(k)\right| \tag{6}$$

Then the final decision is made upon two empirical thresholds($TZ_d = 0.5\ and\ TZ_d = 1$), which are shown in Figure 4, when $TZ_d \le 0.5$ it is diagnosed as healthy state (the roughness level less than 18dB), $0.5 < TZ_d \le 1$ as light fault state (the roughness level between 18dB and 24dB) and $1.5 > TZ_d$ as heavy fault state(the roughness level more than 24dB).

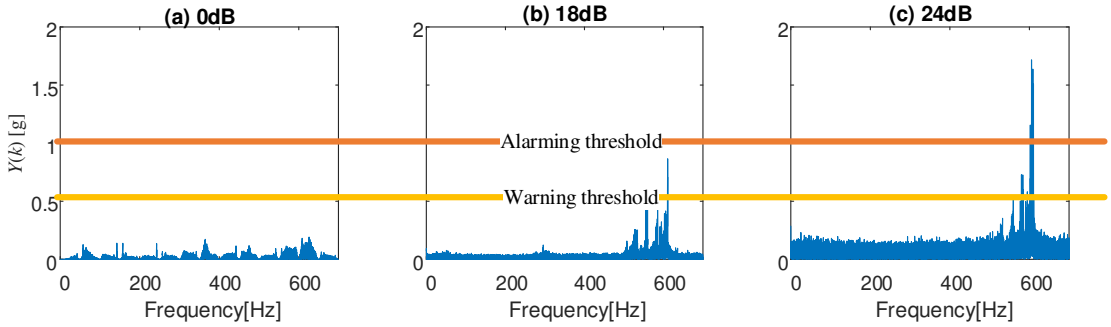

Figure 4 The two diagnosis decision thresholds by the traditional method

However, railway vehicles always run in the presence of fluctuating speed. This is illustrated in Figure 5 which highlights a difference of around 6 km/h within a notional constant speed section of

the route. The traditional DTFT method has limitations on non-stationary signals. Therefore, the misdetection is possible based on the traditional method of DTFT to detect PWRW.

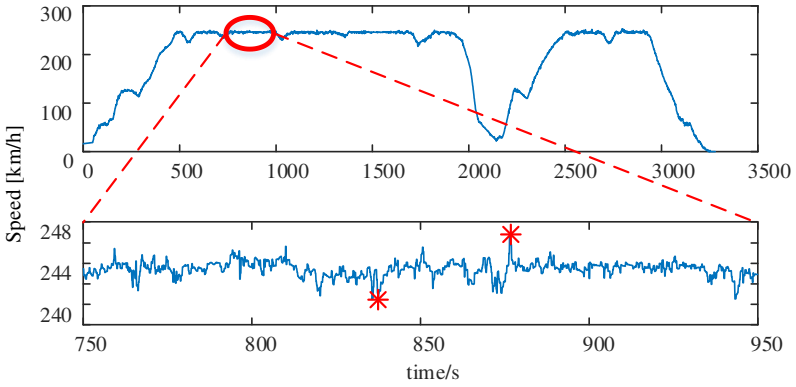

Figure 5 Forward speed data from a real site high-speed train

The passing frequency, f_θ, related to PWRW is between 0Hz to 1400Hz while the forward speed is under 300km/h, which represents a broad range of frequencies[22]. Sets of real fields ABVA data from CRH1, CRH2, CRH3, CRH5, with healthy wheels are shown as Figure 6 both in the time and the frequency domains. From Figure 6, ABVA data have a main frequency band around 500 Hz. Actually, the dominant broadband component around 500 Hz is the natural frequency of wheel-rail coupling[23]. Because the broadband component, the existing DTFT method and other signal decomposition methods, for example the HHT method[23], can also induce misjudgments.

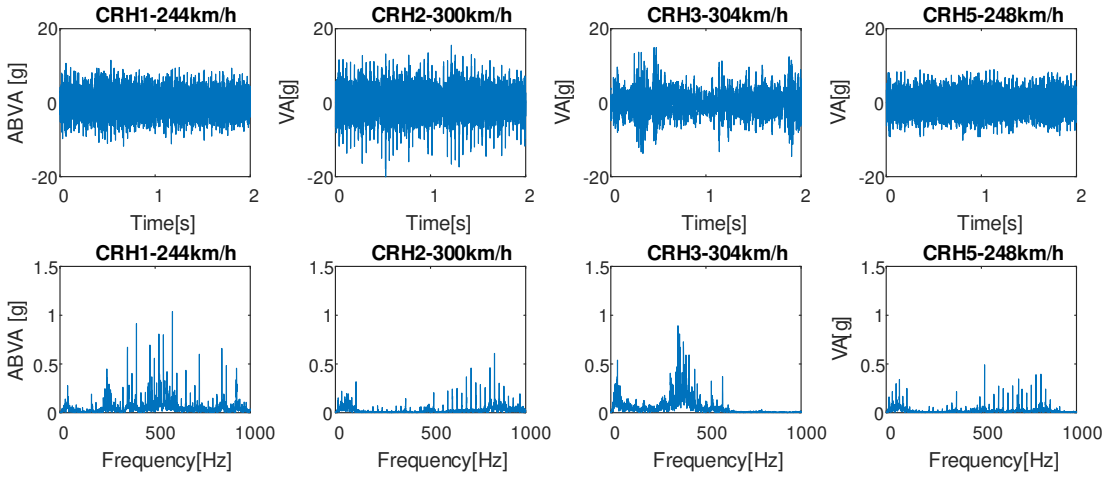

Figure 6 ABVA with health wheels from real sites

3.2. The proposed method

A series of equal impact forces are generated each time when the same area on the wheel tread contacts with standard tracks as the vehicle goes forward[19]. D'Alembert's principle demonstrated that impact forces are proportional to vibration accelerations. Hence, the fault related vibration acceleration component is stationary in wheel angular domain. Based on the mechanism, this paper proposes a on-board detection framework for PWRW combining the ABVA data which is easily available and the ADSAT which can eliminate the angle domain asynchronous and non-coherent random noise. The proposed detection framework, Figure 7, consists of a DAQ system that capture the vehicle speed along with the ABVA data, an outline of the feature extraction methodology and

the process of condition estimation.

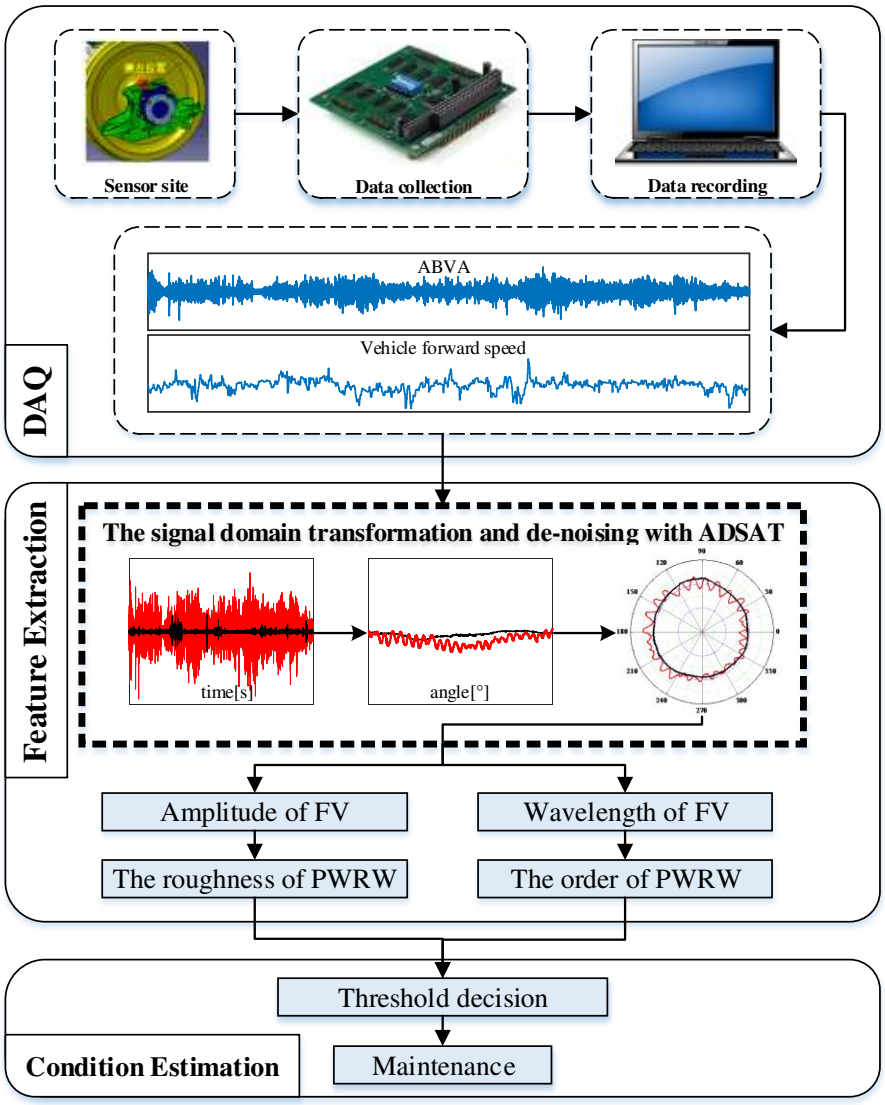

Figure 7 The proposed detection framework

The proposed method is based on the raw vertical ABVA $y(n)$ sampled at f_{vs} Hz and the vehicle forward speed v sampled at f_{ss} Hz. First, obtain the wheel rotational frequency f_0 according to train forward speed v:

$$f_0 = \frac{v/3.6}{\pi D} \tag{7}$$

To transform $y(n)$ from time domain to angle domain, a speed coder is needed. Define the discrete points number of AVBA for each rolling turn is M_r which is easy to solve by:

$$M_r = \frac{f_{vs}}{f_0} \tag{8}$$

Define a vector to describe the wheel vibration condition in the angular domain, which is named the inner-circle vibration of wheel (IVW), remarked as c_r, where r is the number of turns of wheel rolling. As formula (8) shows, M_r is a constant when v is constant. The reconstruction process under variable forward speed $v(n)$ is shown as Figure 8.

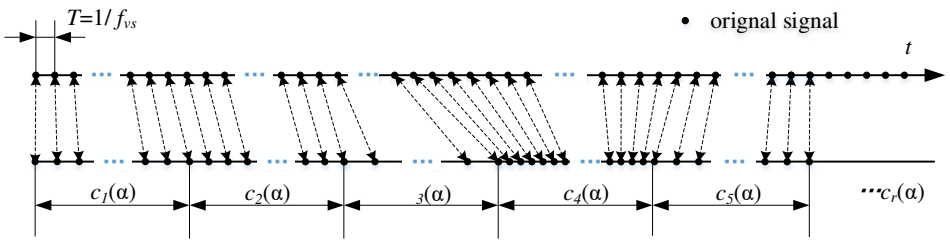

Figure 8 The reconstruction process of the data $y(n)$ to the vector c_r at a variable speed.

After reconstruction, a series of IVW vectors are obtained. ABVA data is noisy because of uncertainties of the operating background, other input disturbances and sampling errors. Even though resampling into angle domain, the IVWs remain too complex to represent the fault of PWRW. The c_r can be divided into three components:

$$c_r(\alpha) = S(\alpha) + NS_r(\alpha) + R_r(\alpha) \tag{9}$$

where $S(\alpha)$ is the angle domain synchronous coherent component which are mainly generated by wheel conditions and define it as the feature vector (FV) to describe the PWRW, $NS_r(\alpha)$ is the angle domain asynchronous coherent components generated by other external excitations, $R_r(\alpha)$ is the non-coherent random noise component. In order to enhance the fault-related component, the asynchronous components and the non-coherent random components should be eliminated. The angle domain synchronous averaging technique (ADSAT) is employed to remove $NS_r(\alpha)$ and $R_r(\alpha)$ by:

$$S(\alpha) = \frac{1}{N/\hat{M}} \sum_{r=1}^{N/\hat{M}} c_r\left[\alpha + 2\pi(r-1)\right] \tag{10}$$

where N is the number of sampled points of ABVA data within a diagnosis step, $\hat{M}$ is the maximum of $M(r)$.

Because the proposed method does not really measure the radial geometry deviation of the wheel, therefore, a health indictor is proposed to represent the roughness level of PWRW, which remains the form of L_θ and replaces the measured radial geometry deviation with the vibrational vector FV, which is:

$$TZ'_d = 20\log_{10}\frac{\hat{Q}}{Q_{ref}} \tag{11}$$

where $\hat{Q}$ is the RMS value of $S(\alpha)$, an empirical reference value Q_{ref} is 0.1 g. We set $TZ'_d = 0$, which means the wheel is healthy, when TZ'_d is less than 0dB. The order of PWRW is the number of the peaks of the feature vector $S(\alpha)$. It is calculated by:

$$TZ'_o = \frac{1}{2}Num(S'(\alpha) == 0) \tag{12}$$

Where $S'(\alpha)$ is the first derivative of $S(\alpha)$, *Num* means the number. In summary, the data flow of the proposed detection method is shown as Figure 9.

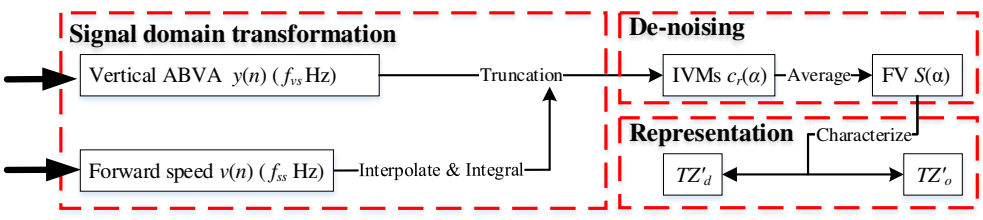

Figure 9 Key steps and data flow within the proposed framework

In order to overcome the negative influence of various operating conditions and increase the robust of the proposed diagnosis algorithm, the diagnosis decision is made by the trend of the indictors for a detection point rather than a certain threshold.

4. Verification of the proposed detection algorithm

The proposed detection framework for PWRW aims at resolving the practical problem. Hence, it should be verified by real field data. However, the noise reduction ability is not easy to be quantified because the calculation of Signal-to-Noise ratio (SNR) needs the power of desired signal component which is difficulted to evaluate in field data. Therefore, the numerical verification is applied to prove the noise reduction ability and the practical verification for the effectiveness of the proposed two indictors.

4.1. Numerical Verification

Based on PWRW's dynamic response mechanism, the ABVA with PWRW can be simulated by:

$$y(n) = \langle (x_1 + x_2), h \rangle + x_3 \tag{13}$$

where x_1 represents the fault excitation of PWRW to the axle-box subsystem h, x_2 represents other harmonic excitations to h, $x_3(n) \sim N(0,2)$ represents the random interference. Specifically:

$$x_1 = A_\theta \sin\left[\theta\left(\frac{v/3.6}{\mathrm{R}}\right)n\mathrm{T} + \varphi_\theta\right] \tag{14}$$

$$x_2 = A_1 \sin\left(2\pi f_1 n\mathrm{T} + \varphi_1\right) + A_2 \sin\left(2\pi f_2 n\mathrm{T} + \varphi_2\right) \tag{15}$$

$$h(n) = A_h e^{-\beta nT} \cos\left(2\pi f_n nT + \varphi_0\right) u(nT) \tag{16}$$

Where sampling time T=10^{-5}s, the total simulated time nT=1s, simulated speed v=250km/h, wheel nominal radius R=0.46m, fault excitation amplitude $A_\theta = 1$, order $\theta = 18$, phase $\varphi_\theta = 0$, harmonic interference excitation amplitude $A_{1,2} = 1$, frequencies $f_{1,2} = 823, 2001$ Hz, phase $\varphi_\theta = 0$, system unit impulse response amplitude A_h=1, attenuation symbol $\beta = 1000$, nature frequency 580Hz. $u(n\mathrm{T})$ is unit step function. The synthesis process is explained by Figure 10. The simulated data in the time domain is shown in Figure 11 and in the frequency domain in Figure 12. The subsystem natural frequency, f_n, is set at 580Hz which is a main natural frequency of the bogie frame [19] and the PWRW order, θ, is set at 18 which is the commonest order of PWRW fault[16].

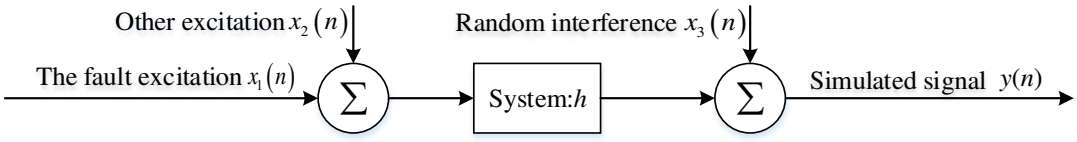

Figure 10 The synthesis process of simulated data

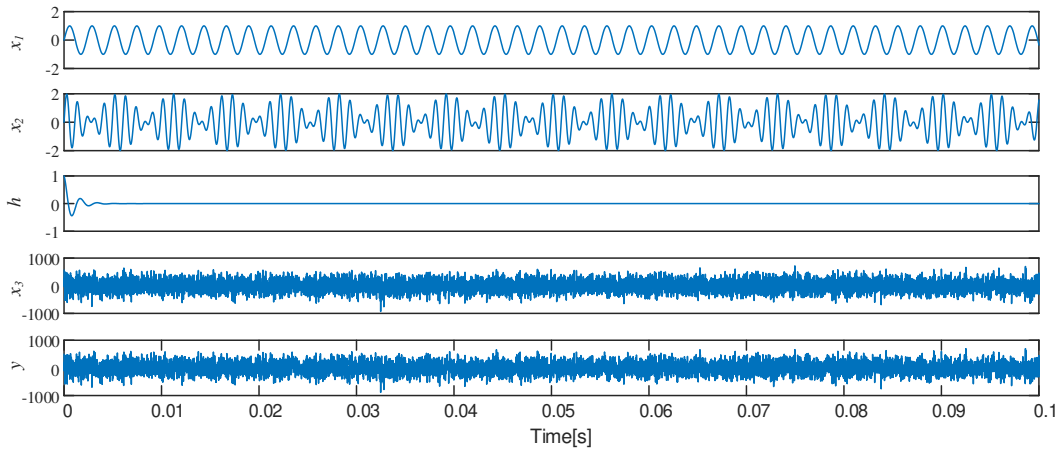

Figure 11 The simulated data in time domain

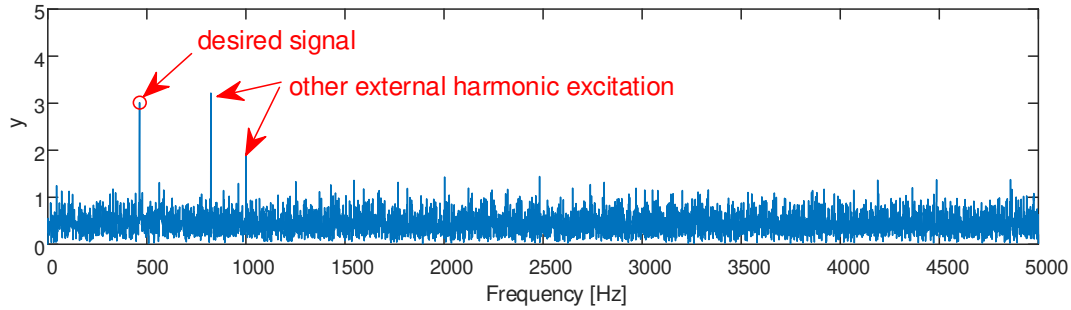

Figure 12 The simulated data y in frequency domain

The ADSAT can enhance the synchronous component and eliminate the asynchronous or the random noise components. Based on the numerical simulation data, the de-noising effect is shown as Figure 13. After processing the FV with ADSAT, the SNR (signal-noise ratio) is improved by a factor of four.

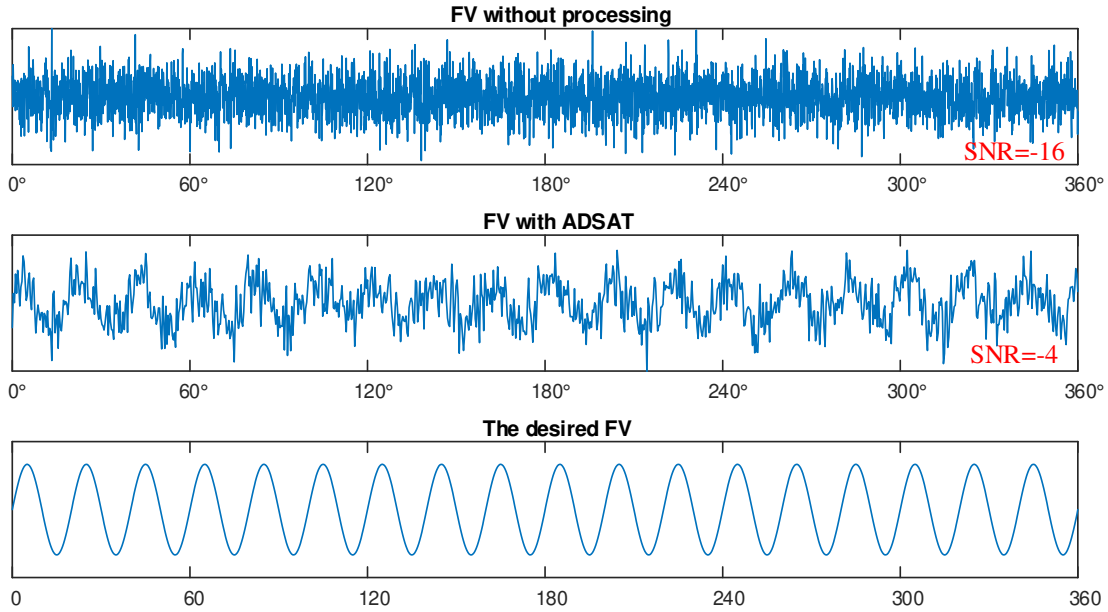

Figure 13 The FVs without processing and with ADSAT

4.2. Practical verification

The proposed method has been used in real filed on high-speed trains. The sensor point in real field are shown in Figure 14.

Figure 14 the monitoring point in real field

Two sets of raw ABVA data from the same axle-box before and after re-profiling are shown as Figure 15. Before re-profiling, the wheel had a serious polygonal wear. The raw data was acquired at the operation mileage of 184,962km. After re-profiling the wheel become healthy. Another raw data was acquired at the operation mileage of 199,286km. The wheel's nominal radius was 0.43m. The vibration data sampling frequency and speed data sampling frequency are 10kHz and 10Hz respectively.

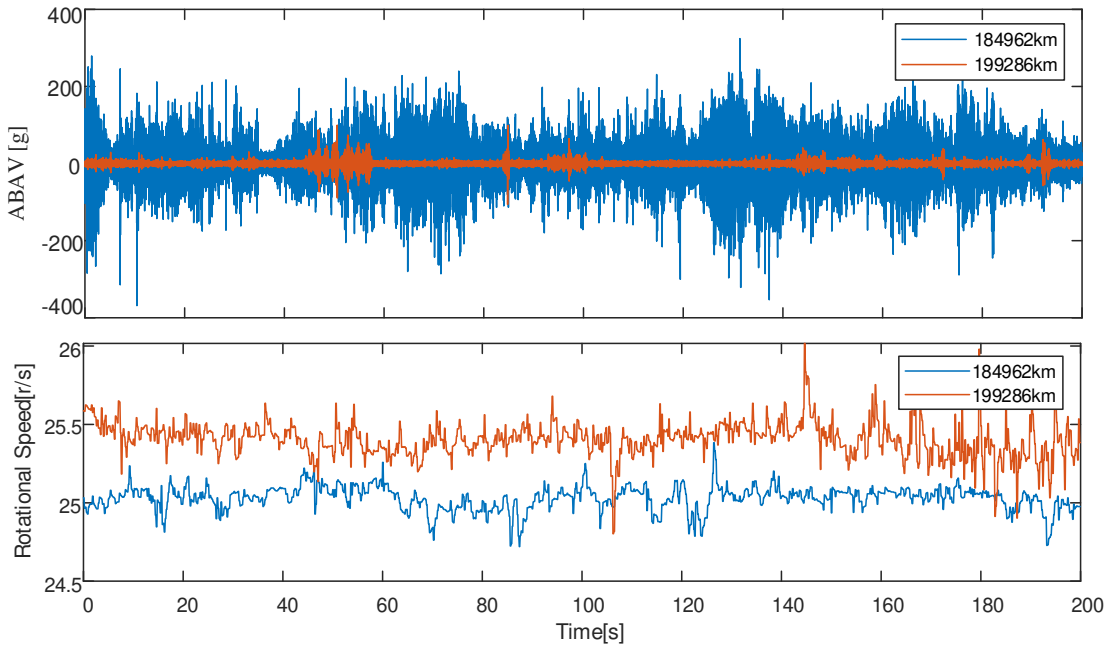

Figure 15 the raw ABVA data and wheel rotational speed from real field

First, the proposed method was used to transform the ABVA data to the angle domain. An L*M matrix is obtained to describe the health status of the wheel, 3 of those IVWs are shown in Figure

16, in which it is easier to recognize the roughness level but still difficult to recognize the order of PWRW.

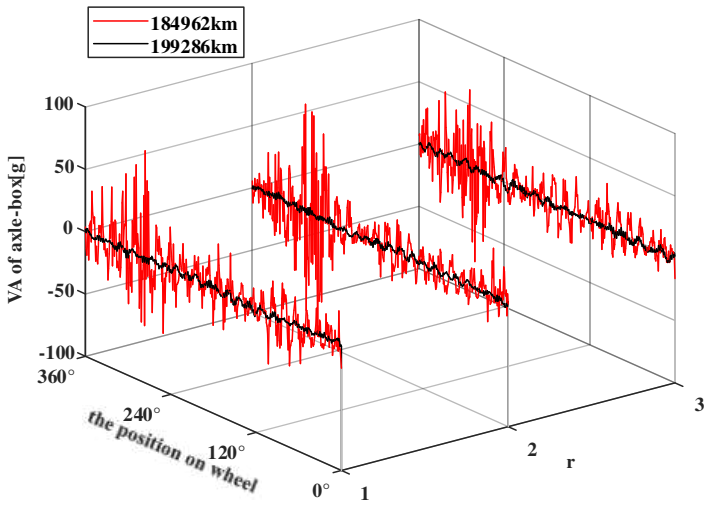

Figure 16 Examples of IVWs from real file data

Hence, the process of IVMs by ADSAT to de-noise and FVs are obtained as shown in Figure 17 (a). The degrees of PWRW are quantified as 7.84 and 0. The effectiveness of the proposed method for detection of the degree parameter of PWRW has been proved. The manual measurement polygonal wear profile, shown as Figure 17 (b), has 24th order PWRW. Compared with the manual measurement result, the proposed method can also detect the 24 wavelengths within one circumference, which means the proposed method is effective to detect the order parameter of PWRW. However, because of properties of vibration data, the proposed method cannot detect the direct component of wheel irregularity, as shown in Figure 17 (b) where there is a strong direct component in the manual measurement result.

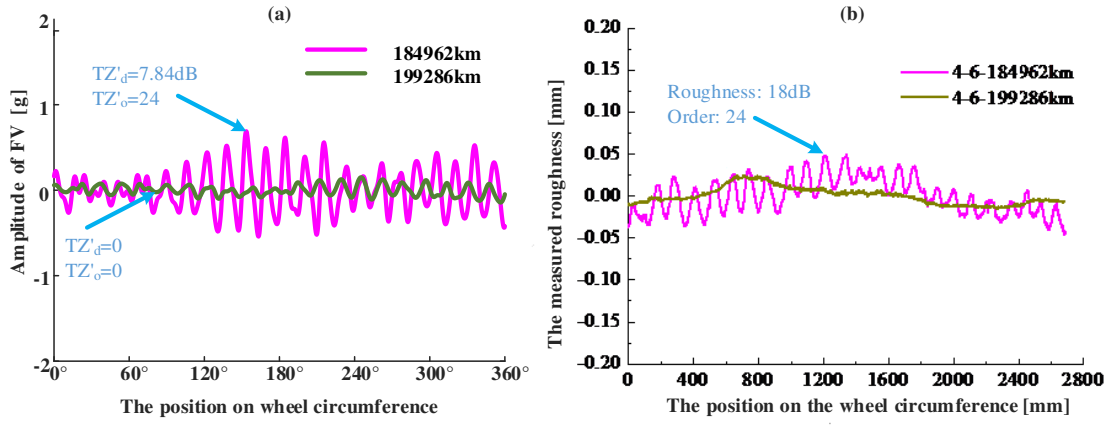

Figure 17 Detection results based on: (a) the proposed method; (b) the manual measurement

DTFT method is typically used to analyze stationary periodic signal. It has limitation to deal with the real field ABVA data. Two sets of one-second data from the real field at fault condition and healthy condition respectively are used to illustrated it. The original ABVA data is shown in the left of Figure 18 and the DTFT result is shown in the right of Figure 18. According to the empirical thresholds mentioned in Figure 4, both are at heavy fault states. Obviously, the traditional DTFT method has a false positive diagnosis. Specially, the diagnosis decision step time usually is one second or shorter to avoid inducing fake harmonic components by DTFT.

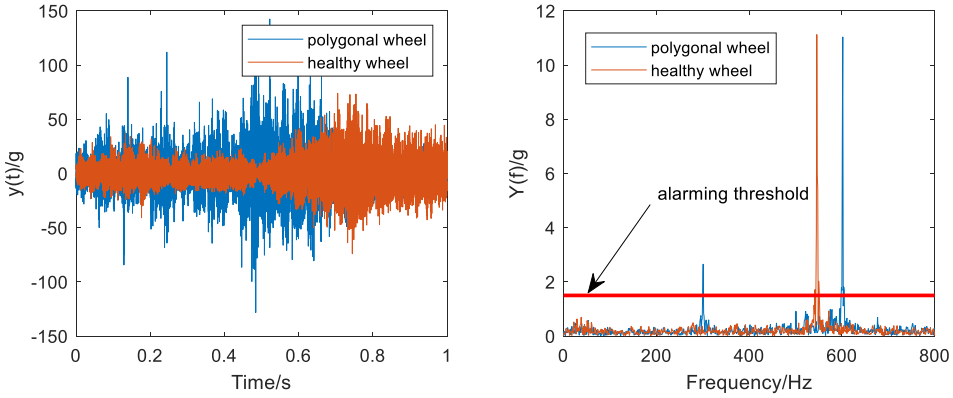

Figure 18 the false positive detection example by the traditional method

5. Conclusions

The traditional on-board detection method for polygon wear of railway wheel based on discrete-time Fourier transform has limitations both on the false positive ratio and the ability to detect the order parameter. In this work, a simple and effective fault detection framework for polygon wear of railway wheel is proposed. It is based on the easily acquired axle-box vibration acceleration data to detect both the level and the order parameters of polygon wear of railway wheel. Since, axle-box vibration acceleration data is usually used to monitor the condition of axle-boxes, it can be accessible as sensor-less method for polygon wear of railway wheel. The de-noising effectiveness is demonstrated using simulated data and the accuracy of the proposed two indictors is proven using two sets of real field data. The proposed method is insensitive to the small-scale speed fluctuation and meets the requirement of on-board detection.

Acknowledgement

This work is partially supported by the National Natural Science Foundation of China (Grant No. 51975487). This work was undertaken at the School of Mechanical Engineering in Southwest Jiaotong University (China). Thanks CRRC Qingdao Sifang Co., Ltd for providing field data. And thanks the China Scholarship Council for supporting Sun Qi to study at Institute for High Speed Rail and System Integration in the University of Leeds, UK, the support Number is 201907000159.

References

[1] Kaper H. P. Wheel corrugation on Netherlands railways (NS): Origin and effects of “polygonization” in particular[J]. Journal of Sound and Vibration, 1988, 120(2): 267-274.

[2] Meywerk M . Polygonalization of railway wheels[J]. Archive of Applied Mechanics (Ingenieur Archiv), 1999, 69(2):105-120.

[3] Meinke P, Meinke S. Polygonalization of wheel treads caused by static and dynamic imbalances[J]. Journal of Sound and Vibration, 1999, 227(5): 979-986.

[4] Nielsen J C O , Johansson A . Out-of-round railway wheels-a literature survey[J]. Proceedings of the Institution of Mechanical Engineers Part F Journal of Rail & Rapid Transit, 2000, 214(2):79-91.

[5] Johansson & C. Andersson. Out-of-round railway wheels—a study of wheel polygonalization through simulation of three-dimensional wheel-rail interaction and wear[J]. Vehicle System Dynamics, 2005, 43(8):539-559.

[6] Xuesong Jin, Lei Wu, Jianying Fang, et al. An investigation into the mechanism of the polygonal wear of metro train wheels and its effect on the dynamic behavior of a wheel/rail system[J]. Vehicle System Dynamics, 2012, 50(12):1817-1834.

[7] J.C.O. Nielsen, A. Mirza, S. Cervello, et al. Reducing train-induced ground-borne vibration by vehicle design and maintenance[J]. International Journal of Rail Transportation, 2015, 3(1):17-39.

[8] Jie Zhang, Guangxu Han, Xinbiao Xiao, et al. Influence of wheel polygonal wear on interior noise of high-speed trains[J]. Journal of Zhejiang University-SCIENCE: A, 2014, 15(12):1002-1018.

[9] Bogacz R , Frischmuth K . On dynamic effects of wheel–rail interaction in the case of Polygonalisation[J]. Mechanical Systems & Signal Processing, 2016, 79(oct.15):166-173.

[10] Nielsen J. Out-of-round railway wheels[M]. Wheel–Rail Interface Handbook. 2009:245-279.

[11] Ding J M , Lin J H , Yi C , et al. Dynamic detection of out-of-round wheels using a comparison of time-frequency feature locatings[J]. Zhendong yu Chongji/Journal of Vibration and Shock, 2013, 32(19):39-43.

[12] Yifan L , Jianxin L , Zhongji L . The Fault Diagnosis Method of Railway Out-of-Round Wheels Using Hilbert-Huang Transform[J]. Journal of Vibration, Measurement & Diagnosis, 2016, 36(4):734-739

[13] Qi S , Bing Z , Yanping L I , et al. Wavelength-fixing mechanisms for detecting the wheel polygon-shaped fault onsite[J]. Journal of Railway ence and Engineering, 2018, 15(9): 2343-2348.

[14] Xiaodi Xu, Jinzhao Liu, Shanchao Sun, et al. Automatic Method for Polygonalization of Wheel Treads Based on Vehicle Dynamic Response[J]. Railway Engineering, 2019, 59(9), 101-105. DOI: 10.3969/j.issn.1003-1995.2019.09.25.

[15] Y.W. Wang, Y.Q. Ni, X. Wang. On-board defect detection of high-speed train wheels by usingBayesian forecasting and dynamic model[J]. Mechanical Systems and Signal Processing, 2020, 139.

[16] Xuesong Jin, Yue Wu, Shuling Liang, et al. Mechanisms and Countermeasures of Out-of-Roundness Wear on Railway Vehicle Wheels[J]. Journal of Southwest Jiaotong University, 2018, 53(1): 1-14.

[17] Nielsen J . Out-of-round railway wheels[J]. Wheel–Rail Interface Handbook, 2009, 50(3): 245-279.

[18] ZHAI Wanming. Vehicle-Track Coupled Dynamics (Fourth Edition) Volume 1[M]. Science press. 2015: 110-111.

[19] Xingwen Wu, Subhash Rakhejaa, Sheng Qu, et al. Dynamic responses of a high-speed railway car due to wheel polygonalisation[J]. Vehicle System Dynamics, 2018, 56(12): 1817–1837.

[20] Bodini, I, Petrogalli, et al. Evaluation of wear in rolling contact tests by means of 2D image analysis[J]. Wear: an International Journal on the Science and Technology of Friction, Lubrication and Wear, 2018.

[21] Alemi, Ali. Condition monitoring approaches for detection of wheel defects[D]. Delft University of Technology, 2019.

[22] Qi Sun, Chunjun Chen, Yanping Li, et al. Extraction of harmonic signatures from broadband noise and its application in the fault diagnosis of wheel polygonalization[C]. Hiroshima: 25th International Congress on Sound and Vibration, 2018, 4047-4053.
[23] Amnon Pieter DE MAN, A survey of dynamic railway track properties and their quality[D]. Delft University of Technology, 2002.

Notation

Nomenclature	
α	Angle domain independent variable, [◦]
β	The attenuation coefficient of the simulated axle-box subsystem function, []
λ_θ	The wavelength of θ^{th} order PWRW, [m]
θ	The order of PWRW, [-]
φ_θ	The initial phase of θ^{th} order PWRW, [rad]
$\varphi_{1,2}$	The initial phases of simulated data, [rad]
A_h	The proportional coefficient of the simulated axle-box subsystem function, [-]
A_θ	Amplitude of θ^{th} order PWRW, [g]
c	The nominal circumference of wheel, [m]
$c_r(\alpha)$	The IVW vector which is the vibration acceleration data of a whole rolling, [g]
D	Wheel diameter, [m]
f_0	Wheel rotational frequency, [Hz]
f_θ	Fault-related frequency of θ^{th} order PWRW, [Hz]
f_n	A natural frequency in the simulated axle-box subsystem function, [Hz]
f_{ss}	Train forward speed sampling frequency, [Hz]
f_{vs}	Axle-box acceleration vibration sampling frequency, [Hz]
g	Acceleration of gravity, 1g≈9.8m/s^2
$h(n)$	The simulated axle-box subsystem unit impulse response, [-]
H	Maximum order usually considered, as usual $H = 40$
L	Distance between points on wheel circumference to a fixed point, [m]
L_θ	Roughness level of θ^{th} order PWRW, [dB]
$M(r)$	Dimension of $c_r(\alpha)$, [-]
$\widehat{M}$	Maximum of $M(r)$, [-]
n	Independent variable of discrete data, [-]
N	The number of ABVA sampled points within a diagnosis step, [-]
$NS_r(\alpha)$	The angle domain non-synchronous coherent components of c_r, [g]
$\hat{Q}$	The RMS of the feature vector $S(\alpha)$, [g]
Q_{ref}	An empirical reference value of $S(\alpha)$, $Q_{ref} = 0.1$g
r	The number of revolution of railway wheel, [-]
$\tilde{r}_\theta$	The RMS in 1/3 octave bands at centre frequency f_θ of PSD of profile deviation, [mm]
r_{ref}	An empirical reference value of $\tilde{r}_\theta$, $r_{ref} = 10^{-3}mm$
R	The number of roll circumference, [m]
$R_r(\alpha)$	The angle domain non-coherent random noise component of $c_r(\alpha)$, [g]
$S(\alpha)$	The proposed feature vector (FC) to describe the PWRW, [g]
t	Time domain independent variable, $t = nT$, [s]
T	Time resolution of ABVA data, [s]
TZ_d	The characteristic to represent the degree of PWRW based on traditional method, [g]
TZ_d'	The characteristic to represent the degree of PWRW based on proposed method, [dB]
TZ_o'	The order parameter of PWRW based on proposed method, [-]

$u(t)$	Unit step function about time t, [-]
v	The speed of vehicle, [km/h]
$x_1(n)$	A simulated PWRW excitation to axle-box subsystem, [-]
$x_2(n)$	A simulated harmonic noise excitation to axle-box subsystem, [-]
$x_3(n)$	A simulated random interference to axle-box vibration response, [-]
$y(n)$	The discrete ABVA data, [g]
$Y(k)$	The result of Fourier Transform of $y(n)$, [g]
$z(t)$	The displacement function of the dynamic excitation of PWRW, [m]

Abbreviations

ABVA: axle-box vibration acceleration
ADSAT: angle domain synchronous averaging technique
CRH1/CRH2/CRH3/CRH5: China Railway High-speed (different EMU in China)
DAQ: data acquisition
DTFT: Discrete-time Fourier transform
FE-SEA: the finite element method and the statistic energy analysis
FSWT: frequency slice wavelet transform
FV: feature vector
HHT: Hilbert-Huang transform
IVW: the inner-circle vibration acceleration vector of the wheel
OOR: out-of-roundness
PSD: power spectral density
PWRW: polygon wear of railway wheel
RMS: root mean square
SNR: signal-noise-ratio